ACS APPLIED MATERIALS & INTERFACES

Research Article

www.acsami.org

Composite Microspheres for Separation of Plasmid DNA Decorated with MNPs through in Situ Growth or Interfacial Immobilization Followed by Silica Coating

Shuai Xu, Xiaojie Song, Jia Guo, and Changchun Wang*

State Key Laboratory of Molecular Engineering of Polymers, Department of Macromolecular Science, and Laboratory of Advanced Materials, Fudan University, Shanghai, 200433, People's Republic of China

Supporting Information

ABSTRACT: Raspberry-like colloidal polymer/magnetite/silica composite microspheres were rationally fabricated based on in situ growth or interfacial immobilization of magnetic nanoparticles (MNPs) onto the polymer matrices and the followed sol−gel coating process. Monodisperse cross-linked poly(styrene-co-glycidyl methacrylate) microspheres were first prepared by surfactant-free emulsion polymerization, followed by surface modification of carboxyl or amine moieties through thiol-epoxy click chemistry. Then the carboxyl-modified microspheres were in situ decorated with MNPs through solvothermal process or chemical coprecipitation reaction. In parallel, incorporation of MNPs onto polymer matrices was also realized by the interaction of amine-modified polymer microspheres with carboxyl-capped MNPs based on the electrostatic interaction. The two pathways for synthesis of the composite microspheres decorated with MNPs were systematically investigated. Furthermore, the composite microspheres were coated with a thin layer of silica through a sol−gel process. The thus-produced magnetic composite microspheres with desirable magnetization (~23 emu/g) served as effective supports for high-payload plasmid DNA enrichment (~17 μg per mg of microspheres), much better than that of the commercial-available sample of SM1−015B (~12 μg per mg of SM1−015B), shedding lights on the potential advantages of the nanoplatforms for separation of bioactive entities.

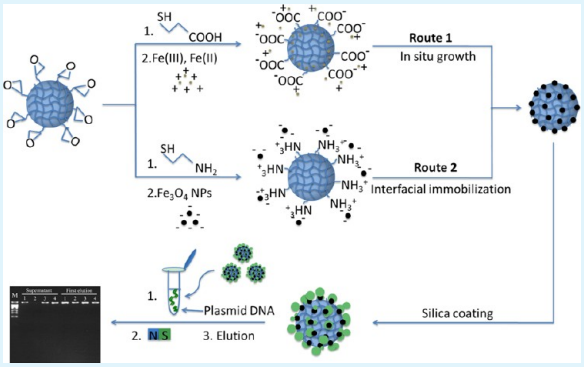

KEYWORDS: *colloidal polymer microspheres, magnetic composite microspheres, sol−gel process, interfacial immobilization, plasmid DNA separation*

1. INTRODUCTION

Colloidal nanoparticles with magnetic property have become increasingly significant for both fundamental studies and technological applications in a wide range of disciplines, including ferrofluids, catalysis, separation of biological entities (e.g., proteins, DNA, and cells), magnetic resonance imaging (MRI), hyperthermia therapy, and magnetically guided targeted drug delivery.[1−10] The magnetic functionality endows the nanomaterials with facile enrichment, separation, and targeting properties, along with in situ monitoring capacity with MRI tomographic methods. Toward the specific requirement, magnetic nanoparticles (MNPs) are elaborately tailored with defined composition, special morphologies and desirable physicochemical properties. Besides, the MNPs also can be designed as building blocks for the composite nanostructures, which offer integrated properties that simple component does not possess.[11−14]

In biorelated fields, efficient detection and separation of specific bioactive entities, such as DNA and proteins, from their original environment are highly required for future analysis.[15−17] For example, the collection and following separation of rare DNA/RNA targets, which have single-base mismatches in a complex matrix is critically important in human disease diagnostics and gene expression studies. Tan and co-workers have fabricated a genomagnetic nanocapturer (GMNC) for the collection, separation, and detection of trace amounts of DNA/RNA molecules.[16] It was demonstrated that GMNC showed highly efficient collection of trace amounts of DNA/mRNA samples down to femtomolar concentrations and confirmed the collected gene products, which favored further gene expression studies. Toward this aim, MNPs/polymer superparamagnetic nanocomposites have been considered as promising candidates because of their facile manipulation of on−off state of magnetization with or without applied magnetic fields and excellent colloidal dispersity, stability, and biocompatibility endowed by polymer components, thereby enabling transportation of targeted biomolecules with a magnetic field.[18,19] Therefore, construction of MNPs/polymer nanocomposites

Received: June 22, 2012
Accepted: August 31, 2012
Published: September 5, 2012

   dx.doi.org/10.1021/am301129n | ACS Appl. Mater. Interfaces 2012, 4, 4764−4775

with tunable structures and optimized structure-dependent properties has aroused tremendous attentions.

Generally, incorporation of MNPs into polymer microspheres could be realized through two principle strategies, in situ growth of MNPs,[20,21] and direct immobilization of MNPs onto polymer microspheres.[22,23] As for the former one, metal salts are initially adsorbed or precipitated inside polymer microspheres, followed by nucleation and formation of MNPs upon increasing pH and temperature.[20] For example, Liu and co-workers reported preparation of chitosan/magnetite composite microspheres based on the adsorbing of iron ions and subsequent in situ formation of the MNPs onto the surface of the templates chitosan microspheres.[24] Similarly, Tang et.al. synthesized ferrimagnetic Fe_3O_4-coated sulfate-stabilized PS microspheres through reduction of Fe(II) by diethylene glycol and followed seeded mediated growth.[25] Besides, immobilization of magnetic nanoparticles onto the surface of polymer microspheres was also an effective tool toward fabrication MNPs/polymer nanocomposites via electrostatic, covalent, and other ways of interaction. For example, Caruso et.al. fabricated magnetic nanocomposites by coating anionic polystyrene (PS) microspheres with magnetite nanoparticle layers alternately adsorbed with polyelectrolyte, the so-called layer-by-layer assembly technique.[26,27] Although considerable progress has been achieved, the reported MNPs/polymer nanocomposites typically suffer from uncontrolled distribution of MNPs around polymer matrix, relatively low saturation magnetization and time-consuming multiple procedures.[11]

Herein, structure-tunable MNPs/polymer microspheres were facilely prepared not only through solvothermal or coprecipitation method for the in situ growth of MNPs but also by heterocoagulation of preformed MNPs onto polymer microspheres as matrix. The MNPs-decorated polymer microspheres were subjected to silica coating for enhancement of the colloidal stability and improvement of the binding affinity between composite microspheres and targeted biological entities of interest. Using the magnetic composite microspheres as supports, plasmid DNA could be effectively enriched and separated from the native solution.

2. EXPERIMENTAL SECTION

2.1. Chemicals and Reagents. Styrene (St) and glycidyl methacrylate (GMA) were purchased from Shanghai Lingfeng Chemical Reagents Co., Ltd., and distilled under reduced pressure before use. Divinylbenzene (DVB, Techn. 80%) was purchased from Aldrich. Potassium persulfate (KPS) and 2-Amino ethanethiol (2-AET) were purchased from Fluka and recrystallized from deionized water. Thioglycolic acid (TGA, 98%) was purchased from Acros Organics (NJ, USA). Iron(III) chloride hexahydrate ($FeCl_3{\cdot}6H_2O$), Iron(II) chloride tetrahydrate ($FeCl_2.4H_2O$), ammonium acetate (NH_4Ac), Trisodium citrate (Na_3Cit), ethylene glycol (EG), aqueous ammonia solution ($NH_3{\cdot}H_2O$, 28%), Ethylenediaminetetraacetic acid (EDTA, pH = 8.0), sodium dodecyl sulfate (SDS), tetraethoxylsilane (TEOS, > 98%), yeast extract (BR), Tris·HCl (pH = 8.0), sodium hydroxide (NaOH), chloroform ($CHCl_3$), acetic acid, potassium acetate, glucose, and anhydrous ethanol were purchased from Shanghai Chemical Reagent Company (China) and used as received. Trypsinase (BR) was purchased from Jinchun Reagent Company and pancreatic RNAase was purchased from Sigma. The marker used in agarose gel electrophoresis was purchased from Hangzhou Axygen Gene Company with the size of 10 kb. The commercial product SM1−015B was purchased from Shanghai Allrun Nano Science and Technology Co., Ltd. Sodium Chloride (NaCl) was purchased from Shanghai Qiangshun Chemical Company. Deionized water (Millipore) of resistivity greater than 18.0 MΩ·cm was used all through the experiments.

2.2. Synthesis of Poly(styrene-co-glycidyl methacrylate) (PSG) Microspheres. PSG microspheres were prepared according to soap-free emulsion polymerization as reported in our group.[28] Briefly 1.5 g of St, 1.4 g of GMA, 0.063 g of DVB (molar ratio = St/GMA/DVB = 58:40:2) and 100 mL H_2O were put into a three-necked flask equipped with a mechanical stirrer and a condenser. The solution was stirred in room temperature, purged with nitrogen for removal of oxygen for 30 min, and heated to 70 °C. Once it reached 70 °C, 0.060 g of KPS dissolved in 2 mL of H_2O was injected to initiate the polymerization under stirring. Gradually, the solution took on opalescent color and became turbid. The reaction was allowed to proceed for another 8 h. The product was harvested with centrifugation, and washed with deionized water for 3 times and then dispersed in water for further use.

2.3. Synthesis of Carboxyl-Terminated PSG Microspheres (PSG-COOH). To obtain carboxylated PSG microspheres, ring-opening reaction was performed through the thiol-epoxy click chemistry.[28] Briefly, 0.09 mL TGA was mixed with 35 mL aqueous solution containing 0.28 g of PSG microspheres. Then the dispersion was transferred into a 50 mL three-necked flask and the pH was adjusted to 11 with little amount of 1 M NaOH solution. The dispersion was stirred vigorously at room temperature overnight. After the reaction, the product was centrifuged, washed with deionized water for 3 times and redispersed in water for further use.

2.4. Synthesis of Amine-Terminated PSG Microspheres (PSG-NH_2). Similarly, 0.28 g as-obtained PSG microspheres were mixed with 0.1 g thioglycol amine chloride into 35 mL of deionized H_2O. The dispersion was transferred into a 50 mL three-necked flask, and the pH value was adjusted to 11 by adding certain amount of 1 M NaOH solution. Then the dispersion was under stirring at room temperature overnight. The as-prepared product was centrifuged, washed with deionized water for 3 times, and redispersed in water for further use.

2.5. Preparation of PSG-COOH@Fe_3O_4 Composite Microspheres through in Situ Growth Route. *2.5.1. Solvothermal Process.* In a typical experiment, 0.054 g of $FeCl_3{\cdot}6H_2O$ and 0.12 g of NH_4OAc was dissolved in 35 mL of EG under sonication for 10 min to ensure homogeneity. Then the solution was poured into three-necked bottle and stirred vigorously under the protection of N_2. And 2 mL water solution containing 0.054 g of PSG-COOH microspheres was dropped slowly into the above solution. Further, the mixed solution was heated to 160 °C and stirred for 40 min. Then the orange colored solution was transferred to a Teflon-lined stainless autoclave (50 mL capacity), heated to 200 °C, and maintained for 16.5 h. Then the brownish product was rinsed several times with ethanol and water to remove the excess polymer microspheres and the solvent. The product was separated from supernatant with magnet ($Nd_2Fe_{14}B$, 1.2 T) during each washing step and then stored in ethanol for further use. For the preparation of citric acid stabilized PSG-COOH@Fe_3O_4 microspheres, the experiment process was the same as aforementioned, apart from the addition of 10 mg of sodium citrate into the solution before reaction.

2.5.2. Coprecipitation Reaction. Typically, 2.8 g $FeSO_4$ and 0.04 g $FeCl_3$ were added into 50 mL of aqueous solution containing 0.1 g of PSG-COOH. The dispersion was ultrasonicated for 3 min to ensure homogeneity. Then the dispersion was transferred into a 100 mL three-necked flask, stirred vigorously under N_2 atmosphere. The stirring process was allowed to proceed at room temperature overnight. After it, excess iron ions were washed with water and isolated by centrifugation. Then the polymeric microspheres absorbing iron ions were redispersed in 10 mL of water and stirred vigorously under N_2 atmosphere. Next, 10 mL of 3 M NaOH solution was added into the dispersion and the color changed into black immediately upon addition of NaOH solution, indicative of formation of magnetite nanoparticles. The coprecipitation reaction was performed for 2 h at 60 °C. Then the brownish black product was washed with water for 3 times and isolated by an external magnet.

Scheme 1. Schematic Illustration of the Preparation of PSG@Fe_3O_4@SiO_2 Composite Microspheres Based on the in Situ Growth Route

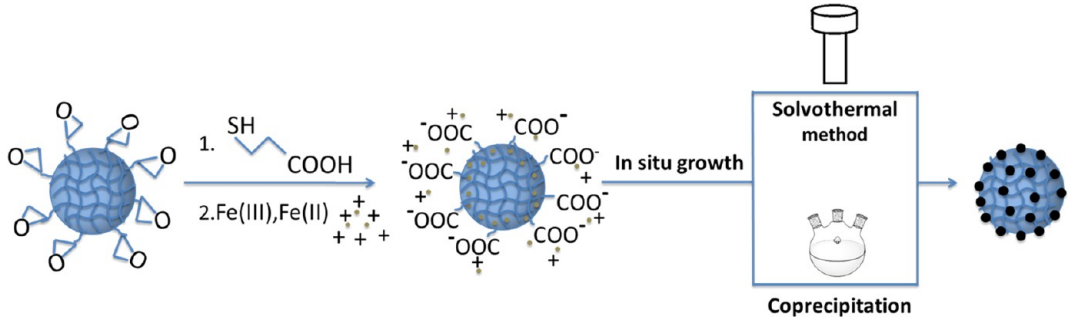

2.6. Preparation of PSG-NH_2@Fe_3O_4 Composite Microspheres through Interfacial Immobilization Route. Magnetite nanoparticles were prepared through coprecipitation reaction of Fe(III) and Fe(II) chloride. Typically, 10.8116 g $FeCl_3 \cdot 6H_2O$ (0.04 mol) and 3.976 2 g of $FeCl_2 \cdot 4H_2O$ (0.02 mol) were added into 100 mL of aqueous solution and ultrasonicated for homogeneity. The dispersion was stirred vigorously at room temperature under N_2 atmosphere, and 50 mL amount of 10 M NaOH solution was injected into the dispersion slowly within 30 min, during which the color changed into black, indicating magnetite nanoparticles formed. The stirring process was allowed to proceed for 1 h. Then the temperature was elevated to 90 °C for another 2 h of stirring. After cooling to room temperature, the product was isolated by an external magnet and washed with acidic water several times until the supernatant was neutral. Then the product was added into 100 mL of sodium citrate solution (0.3 M) and stirred for 30 min at 90 °C under N_2 atmosphere. After it was cooled to room temperature, the product was separated by an applied magnet and washed with excess amount of acetone. Finally, the purified product was dispersed in 50 mL water and stirred vigorously at 80 °C for removal of remnant acetone.

For the preparation of PSG-NH_2@Fe_3O_4 microspheres, 0.5 mL of PSG-NH_2 aqueous solution(solid content 3.22%) was added dropwise into 25 mL solution of citrate-acid-modified magnetic fluids(solid content, 0.021%), and the mixture was incubated for 30 min. Then the dispersion was centrifuged several times to remove the supernatant until it became transparent, excluding nonabsorbed bare Fe_3O_4 nanoparticles.

2.7. Silica Coating onto the PSG@Fe_3O_4 Microspheres. The silica-coating process was performed according to the modified Stober process.[29] Typically, 0.010 g of as-prepared PSG@Fe_3O_4 microspheres (PSG-COOH@Fe_3O_4 or PSG-NH_2@Fe_3O_4) were dispersed in a mixture of 9 mL of water, 40 mL of ethanol, and 1 mL of 28 wt % aqueous ammonia solution. The solution was ultrasonicated homogeneously for 10 min, followed by addition of 0.2 g TEOS. Then the reaction further proceeds for 45 min under sonication at ice bath. The obtained light brownish product was washed repeatedly with ethanol and water to remove the excess $NH_3 \cdot H_2O$ and TEOS, separated by magnet, and redispersed in ethanol. The purified product was dried under vacuum for further use.

2.8. Plasmid DNA Extractions. The *Escherichia coli* colony was disinfected and cultured in LB medium at 37 °C overnight before DNA extraction. The colony medium was centrifuged to remove the supernatant and 3 mL of solution I (50 mM glucose, 25 mM Tris.HCl, pH 8.0, 10 mM EDTA, pH 8.0) was added into it for 10 min of mixing. Then 6 mL solution II (0.4 M NaOH, 2% SDS, v/v = 1:1) was added into the above solution, shaking for homogeneity, and placed onto the ice for 5 min. After that, 4.5 mL ice-cold solution III (a mixture of 60 mL potassium acetate solution (5 M), 11.5 acetic acid, and 28.5 mL water) was added and placed onto the ice for 15 min. Then the dispersion was centrifuged and the supernatant was transferred to another tube, to which 15 mL of phenol and chloroform (v/v = 1:1) was added and shaked for homogeneity, followed by centrifugation. The supernatant was divided into two parts, to each one 2 times volume of anhydrous ethanol was added and laid for 5−10 min. Then the dispersion was again centrifuged and the supernatant was removed thoroughly with an aid of absorbent paper. The plasmid DNA precipitates was carefully washed by 70% ethanol solution, centrifuged to remove the impurities and dried in the air. To each tube 2.25 mL TE buffer (10 mM Tris-HCl, 1 mM EDTA pH = 8.0) containing 20 μg/mL Pancreatic RNAase was added and the plasmid DNA was kept at −20 °C for further use.

2.9. Plasmid DNA Separation. Thirty micrograms of plasmid DNA was added into 300 μL of buffer solution (2 M NaAc, 6 M Gu-HCl, pH = 5.0) containing 1 mg of PSG@Fe_3O_4@SiO_2 microspheres, and the mixture was ensured homogeneity by slight shaking. Then magnetic microspheres were driven by an applied magnet to the side wall of the tube. After that, the supernatant was extracted into the 1.5 mL DNA preparation tube, dried in vacuum, and added by 500 μL buffer W1. The dispersion was washed twice with 700 μL buffer W2 (0.1 M NaCl, 20 mM Na_2HPO_4, 80% EtOH, pH = 6.5) and separated by centrifugation. Then 60 μL eluent (5 mM Tris-HCl, pH = 8.0) was added to elute DNA. Then elution process was repeated once. Concentration of plasmid DNA was determined through the ultraviolet absorbance at 260 nm (A_{260}).

2.10. Agarose Gel Electrophoresis Experiments. The recovered plasmid DNA was confirmed by 1.2% agarose gel electrosphoresis, and the gel was stained with ethidium bromide (EB). Two microliters of loading buffer was mixed with 1.5 μL sample solution for homogeneity. All the samples and the standard DNA Marker (300−10000 bp) were added into the agarose gel for 20 min electrophoresis, with the voltage of 100 V and current of 400 mA.

2.11. Characterization. Transmission electron microscopy (TEM) images were obtained on an H-600 (Hitachi, Japan) transmission electron microscope at an accelerating voltage of 75 kV. High-resolution Transmission electron microscopy (HRTEM) images were taken on a JEM-2010 (JEOL, Japan) transmission electron microscope at an accelerating votage of 200 kV. Samples dispersed at an appropriate concentration (1−5 mg/mL) were cast onto a carbon-coated copper grid. Scanning electron microscopy (SEM) images were performed using a TS-5136MM (TESCAN, Czech) scanning electron microscope at an accelerating voltage of 20 kV. Samples dispersed at an appropriate concentration were cast onto a glass sheet at room temperature and sputter-coated with gold. Powder X-ray diffraction (XRD) patterns were collected on a D8 advance (Bruker, Germany) diffraction meter with Cu KR radiation at λ = 0.154 nm operating at 40 kV and 40 mA. Magnetic characterization was carried out with a vibrating sample magnetometer on a Model 6000 physical property measurement system (Quantum Design, USA) at 300 K. Hydrodynamic diameter (D_h) and ζ-potential measurements were conducted with a Nano ZS Zetasizer (model ZEN3600, Malvern Instruments) using a He−Ne laser at a wavelength of 632.8 nm. Optical micrographs were obtained from Olympus BX51microscope. UV−vis absorption spectra were measured on a Powerwave XS2 spectrophotometer (Gene Company). Agarose gel elecrophoresis was conducted at Tanon EPS-100 nucleic electrophoresis apparatus with Tanon-2500 automatic electrophoresis images managing system.

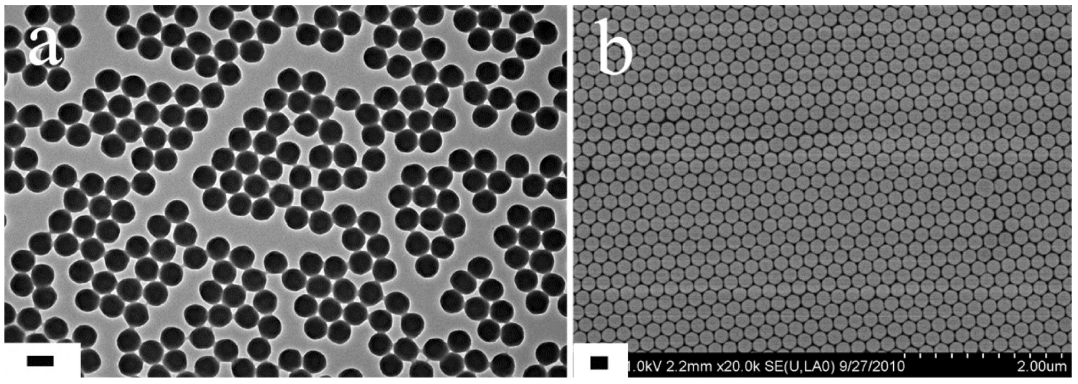

Figure 1. (a) TEM and (b) SEM image of PSG-COOH microspheres. All scale bars are 200 nm.

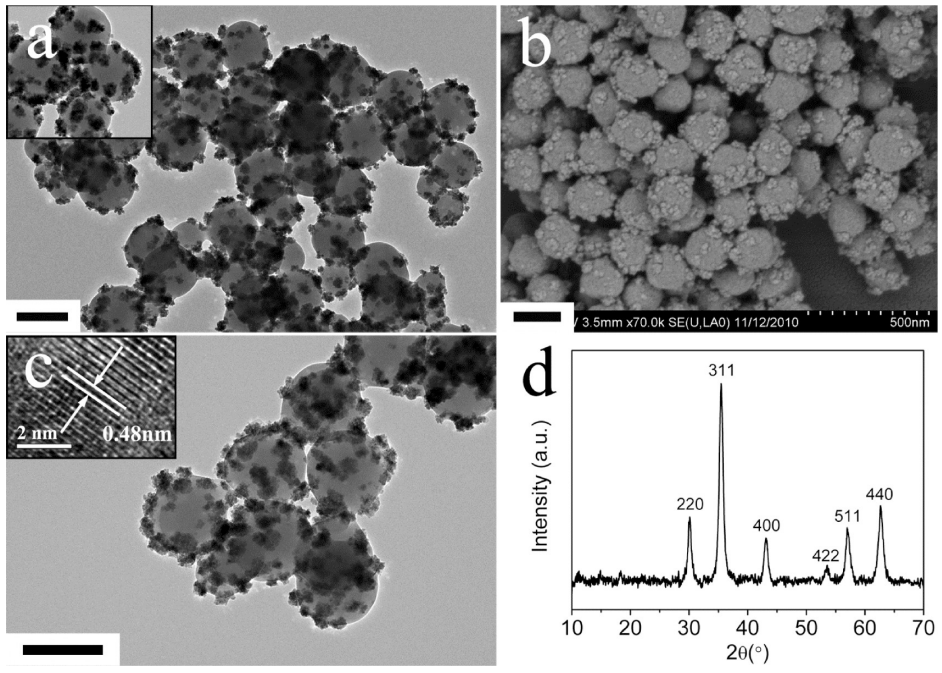

Figure 2. (a, c) TEM images, (b) SEM image, and (d) powder XRD pattern of PSG-COOH@Fe_3O_4 composite microspheres. Inset in panel c is a HRTEM image of MNPs. All scale bars are 200 nm.

3. RESULTS AND DISSCUSSION

3.1. Preparation of PSG-COOH@Fe_3O_4 Composite Microspheres through in Situ Growth Route. Incorporation of magnetite nanoparticles (MNPs) into polymer matrix could be rationally realized either by in situ nucleation and growth or interfacial immobilization route. As discussed, the in situ formation method referred to the procedure that iron resource is first absorbed onto the surface of polymer latex, followed by in situ nucleation and growth of MNPs, finally forming polymer/Fe_3O_4 composite microspheres. Through carefully manipulation of the reaction conditions, the nanostructures of the resultant microspheres could be tuned accordingly. In the experiments, the two pathways including solvothermal process and chemical coprecipitation reaction were employed to facilitate nucleation and growth of MNPs through in situ growth route, and the synthetic procedure for PSG-COOH@Fe_3O_4 composite microspheres from the two routes is schematically illustrated in Scheme 1.

PSG microspheres were prepared by surfactant-free seeded emulsion polymerization with styrene (St) and glycerol methacrylate (GMA) as monomers, KPS as an initiator, and DVB as a cross-linking agent to keep the microspheres stable during the reaction process. Dynamic light scattering (DLS) results showed that the average diameter of the as-made microspheres was 254 nm with a narrow size distribution of PDI = 0.075 (PDI, particle dispersion index). Then TGA was applied to introduce carboxyl groups through ring-opening reaction between thiol and epoxy groups of the microspheres,[28] and the reaction was facilely performed overnight under magnetic stirring at elevated temperature of 50 °C. After carboxyl modification, the ζ-potential of the microspheres was measured to decrease obviously from −27.4 to −45.2 mV, reflecting the successful functionalization of carboxyl functionalities. To be noted, unmodified PSG microspheres were negatively charged mainly attributed by the surface adsorbed anionic initiator persulfate ($S_2O_8^{2-}$) residues after the emulsion polymerization. As shown in the Figure 1, the as-prepared PSG-COOH microspheres were spherically shaped, uniform in size and exhibited excellent aqueous dispersity and stability.

3.1.1. In Situ Growth of MNPs via Solvothermal Method. The PSG-COOH microspheres had a strong affinity toward iron species through coordination or electrostatic interaction,

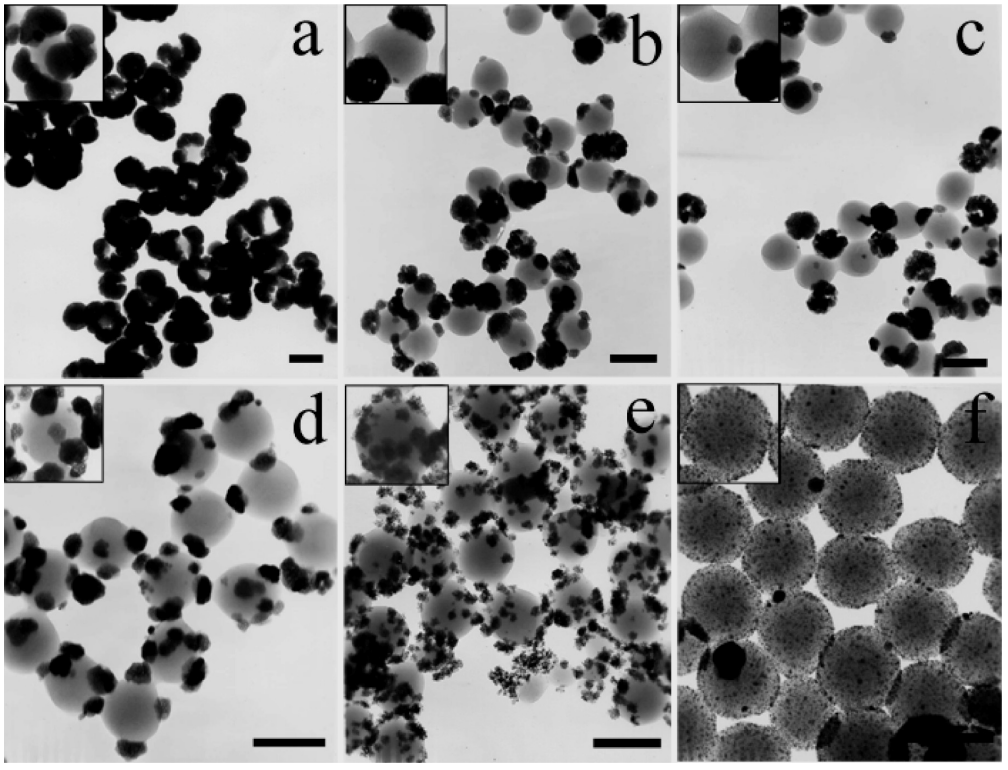

Figure 3. TEM images of PSG-COOH@Fe_3O_4 microspheres through solvothermal process with decreased $FeCl_3$ to PSG-COOH weight ratio of (a) 4:1, (b) 2:1, and (c) 1:1, insets are enlarged images, and sodium citrate feeding amount of (d) 5 mg, (e) 10 mg, and (f) 25 mg (ratio was 1:1). The PSG-COOH amount is kept the same at 54 mg. Inset with border are the enlarged images, all scale bars are 200 nm.

promoting the adsorption of iron ions onto their surface for further heterogeneous nucleation and growth of magnetic nanoparticles in the so-called in situ growth mode.

Solvothermal process, a traditional powerful method for the preparation of magnetic clusters,[30−32] was applied to grow MNPs onto the polymeric matrix. As we know, solvothermal reaction typically occurs under high pressure and elevated temperature (>200 °C) to facilitate the formation of magnetic clusters with enhance saturation magnetization.[8,32] Herein, taking iron(III) chloride hexahydrate as iron resource, ammonia acetate as alkaline resource, and sodium citrate as stabilizers, the cross-linked PSG-COOH microspheres were mixed with above components in ethylene glycol (EG) under magnetic stirring at elevated temperature of 160 °C, during which the coordination interaction occurred thoroughly. In this process, the surface-coordinated iron species had an intendency to be changed to $Fe(OH)_3$ in the alkaline conditions, and they were partially reduced to $Fe(OH)_2$ by EG, meanwhile dehydration reaction took place gradually. Subsequently, the above mixture was transferred into sealed autoclaves at 200 °C for the heterogeneous nucleation and growth of MNPs in the reducing environment. Figure 2a showed a representative TEM image of as-prepared PSG-COOH@Fe_3O_4 composite microspheres. The PSG-COOH latex could maintain structural integrity and uniformity in size after solvothermal reaction due to the existence of cross-linker DVB. It could be clearly distinguished that black MNPs sized around 5−10 nm had grown onto the surface of polymeric microspheres, and the density was nearly uniform in each microsphere. Accordingly, the smooth and spherical microspheres were covered by many small nanoparticles, resulting in rough, coarse, and raspberry-like morphology (Figure 2b). In sharp contrast, using unmodified epoxy-capped polymeric microspheres as seeds, the coverage of MNPs was far from satisfactory with a considerable proportion of individual MNPs in the identical experimental conditions (Supporting Information Figure S1). Thereby, carboxyl functionalization served as a necessary step to direct the attachment of MNPs onto polymeric matrix.

Besides, further investigations were performed to verify the magnetite phase of the as-prepared MNPs. A high-resolution TEM image taken from the arrowed area in Figure 2c showed the periodic fringe spacing of the crystallographic planes, which was estimated to be approximate 0.48 nm, consistent with the interplanar spacing between the (111) lattice planes of the Fe_3O_4 crystals (Figure 2c, inset). Additionally, the powder X-ray diffraction (PXRD) pattern of the product in Figure 2d revealed that, according to JCPDS 75-1610, the characteristic peaks were accurately indexed to the cubic structure of Fe_3O_4 crystals without any other impure phases.[32,33]

To finely adjust the grafting density and size of MNPs, the dosage of iron resource and stabilizer sodium citrate were investigated systematically. Figure 3a−3c showed the PSG-COOH@Fe_3O_4 composite microspheres with decreased weight ratio of iron chloride to polymer microspheres. At a high ratio of 4:1, obviously, several magnetic nanoparticles with large sizes (∼180 nm) could cover onto the polymer latex, forming big nodules onto the surface (Figure 3a). However, with reduced ratio to 2:1 and 1:1, the surface-grown MNPs were decreased both in number and in size (Figure 3b and 3c, ∼110 nm and ∼95 nm). Besides, one could find that a majority of MNPs were nearly hemisphere in shape rather than entire spherical particles, which meant that MNPs had nucleated and grown heterogeneously from the matrix at the beginning instead of attachment after homogeneous growing in EG. Thereby, the

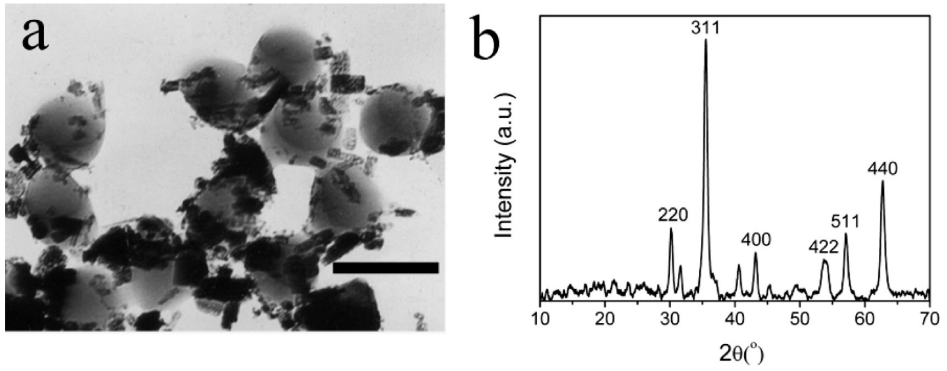

Figure 4. (a) TEM image and (b) powder XRD pattern of PSG-COOH@Fe_3O_4 composite microspheres based on the coprecipitation reactions. Scale bar is 200 nm.

Scheme 2. Schematic Illustration of Preparation of PSG@Fe_3O_4@SiO_2 Composite Microspheres via the Interfacial Immobilization Route

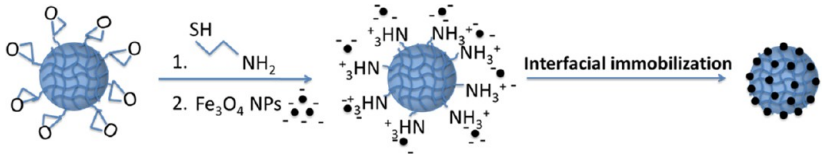

formation of magnetic composite microspheres was dominantly based on the in situ seeded-mediated growth process.

Besides, stabilizers also serve as an effective tool in controlling the morphology of resultant microspheres. Basically, the existence of stabilizer sodium citrate influenced the size and distribution of MNPs on the surface. Compared with the microspheres prepared without addition of sodium citrate (Figure 3a–c), addition of stabilizer could make the as-prepared MNPs much more uniform and small in size (~60 nm, Figure 3d). With a 10 mg dosage of sodium citrate, high coverage of MNPs with reduced size can be attained, resulting in core–satellite structures with relatively enhanced specific surface area (~40 nm, Figure 3e). Further increasing the amount of sodium citrate, the magnetic dots sized around several nanometers covered the whole surface area of the polymer microspheres (~15 nm, Figure 3f). The average sizes of MNPs for samples in Figure 3 were listed in Supporting Information Table S1. In the circumstances with stabilizers, polymeric microspheres could adsorb many citric ions through swelling process in the pretreatment at 160 °C, endowing more carboxyl groups onto their surfaces, which served as anchoring sites to iron species through coordination interaction. Thus, more nucleation sites on the surface were available for the formation of MNPs. Moreover, the initially formed MNPs were stabilized by carboxyl groups of citric acid and thereby subsequent growth of MNPs was limited due to the electrostatic repulsion provided by free carboxyl groups. To be more specific, ζ-potential measurements revealed that the microspheres were more negatively charged along with more addition of sodium citrate, from −15.7 to −25.1 to −36.2 mV. On the basis of the above discussion, MNPs would be much smaller in size and more dissipated over the polymeric surfaces with increased amount of stabilizers.

Polymeric microspheres covered with small MNPs are definitely beneficial for further biomolecules separation because of the relative large surface area for higher targets loading capacity. Meanwhile, MNPs with decreased size will lead to weakened saturation magnetization, unavoidably lowering down the separation efficiency. Based on it, a desirable biomolecule separation nanoplatform required both high magnetization for facile magnetic manipulation and enough surface areas for payload carrying. Thus an appropriate amount of stabilizers (about 10 mg) was used in the experiments. Besides, it was also worth notice that composite microspheres stabilized by sodium citrate were well dispersed and maintained prolonged stability in aqueous solution (Supporting Information Figure S2).

3.1.2. In Situ Growth of MNPs via Coprecipitation Reaction. Apart from the solvothermal procedure, chemical coprecipitation based in situ growth of MNPs was also investigated to prepare PSG-COOH@Fe_3O_4 microspheres. Basically, chemical coprecipitation reaction was a traditional pathway to fabricate magnetic nanoparticles in a facile and straightforward manner,[34,35] especially compared with the solvothermal process. In the process, the carboxyl-enriched microspheres were immersed in a mixed aqueous solution of abundant Fe(II) and Fe(III) ions overnight, ensuring an enough amount of iron resources adsorbed onto the surface via combined coordination and electrostatic interaction. Then, excess iron ions were washed away thoroughly to avoid subsequently homogeneous nucleation of MNPs, which were difficult for further magnetic separation from composite microspheres. Finally, surface-anchored iron ions were treated with alkaline, dehydrated, and nucleated to form MNPs.

The structures of PSG-COOH@Fe_3O_4 microspheres through coprecipitation reactions were shown in Figure 4a. One could find that the MNPs sized around 50 nm (Supporting Information Table S2) grown from the polymer matrix and assembled onto the surface to form composite structures. Powder XRD pattern in Figure 4b further verified the as-prepared nanoparticles, which were ascribed to cubic structure of Fe_3O_4 crystals according to JCPDS 75-1610. However, the two peaks centered on 32° and 41° shown in Figure 4b could be well indexed to the (104) and (113) lattice planes of the α-Fe_2O_3 structure, according to JCPDS No. 80-2377.[30] It is probably that a small fraction of α-Fe_2O_3 formed

dx.doi.org/10.1021/am301129n | ACS Appl. Mater. Interfaces 2012, 4, 4764–4775

during the coprecipitation process. In the control experiment, PSG-COOH microspheres without prior soaking in iron solution were used as seeds to grow MNPs. However, little MNPs were found to stay on the surface of polymer micropsheres, indicative of insufficient interaction between iron ions and carboxyl groups, together with fast nucleation of MNPs in the coprecipitation process. Consequently, such pretreatment was necessary to allow complete interaction between iron ions with carboxyl groups of polymer microspheres.

3.2. Preparation of PSG-NH_2@Fe_3O_4 Composite Microspheres through Interfacial Immobilization Route. Considering from another angle, construction of the polymer/magnetite composite microspheres also could be realized through a simple and straightforward way, involving directly attaching of MNPs with suitable functionalities onto the surface of polymer microspheres (Scheme 2). Such interfacial immobilization method should be based on the strong affinity between MNPs and polymer microspheres. According to the above consideration, carboxyl-functionalized MNPs were applied to cover onto the surface of amine-modified polymer microspheres via electrostatic interaction. Hence, the PSG microspheres were modified with 2-aminoethanethiol (2-AET) to introduce $-NH_2$ groups onto the surface. Then the PSG-NH_2 microspheres were added in aqueous solution of carboxyl-capped MNPs derived from coprecipitation method, followed by stirring for 30 min to promote electrostatic interaction and form raspberry-structured PSG-NH_2@Fe_3O_4 microspheres.

The effect of the $-NH_2$ contents on the final structures of the obtained composite microspheres was investigated. By using different molar ratio of GMA (20%, 40%, or 60%, denoted as PSG-20, PSG-40, and PSG-60, respectively) in the emulsion polymerization, the surface-capped epoxy contents in the resultant polymer microspheres were changed accordingly. Thereby, after treating with excess amount of 2-AET, the $-NH_2$ contents of the microspheres with various GMA content were also altered. The data was shown in Table 1, the PSG microspheres synthesized with various GMA contents were sized around 250−320 nm. ζ-Potential measurements revealed that these microspheres were negatively charged of around −30 mV, because of the remnant initiator ions as mentioned above. Upon 2-AET modification, the sizes of the microspheres were slightly enlarged probably attributed by the enhanced hydrophilicity from epoxy to amine groups. More importantly, amine-modified microspheres were positively charged and the ζ-potential changed from +2.3 to +21.6 and to +40.9 as the GMA contents increased from 20% to 40% and to 60%, respectively. In other words, the $-NH_2$ concentration on the surface of the PSG microspheres was positively correlated with the GMA contents.

Table 1. Size, PDI, and ζ-Potential of PSG Microspheres with Different GMA Contents and Followed $-NH_2$ Functionalization

sample	size (nm)	PDI	ζ-potential (mV)
PSG-20	314 ± 28	0.049 ± 0.012	−32.0 ± 3.1
PSG-40	273 ± 19	0.003 ± 0.008	−29.0 ± 2.6
PSG-60	254 ± 37	0.075 ± 0.020	−27.4 ± 0.8
PSG-20-NH_2 (MP-20)	339 ± 64	0.091 ± 0.130	+2.3 ± 2.1
PSG-40-NH_2 (MP-40)	305 ± 29	0.089 ± 0.074	+21.6 ± 1.8
PSG-60-NH_2 (MP-60)	278 ± 24	0.077 ± 0.031	+40.9 ± 5.8

Citrate-acid-stabilized MNPs were prepared from coprecipitation as reported in our groups.[35] The MNPs were around 32 nm in size (Table S2) as shown in the TEM image (Figure S3), and owned negative charges as much as −52.3 mV, which was desirable for electrostatic interaction with positively charged PSG-NH_2 microspheres. When MNPs interacted with PSG-20-NH_2 microspheres with +2.3 mV surface charge, little amounts of MNPs could adsorb onto the surface of amine-terminated PSG microspheres as displayed in Figure 5a, due to the weak and insufficient electrostatic interaction between them. As the surface charges increased to +21.6 mV, obviously, more MNPs could be incorporated into the PSG-NH_2 surface (Figure 5b), revealing the enhanced electrostatic interaction in such case. Furthermore, MNPs tended to cover the whole polymeric microspheres with further increased the surface charge of +40.9 mV (Figure 5c).

Furthermore, powder XRD patterns of the three composite microspheres in Figure 6a revealed that all peaks could be well indexed to the magnetic cubic structure of magnetite (JCPDS No. 75-1610). The intensity of the characteristic peaks was strengthened as the weight fraction of MNPs increased. In addition, it could be verified from the TG curves (Figure 6b) that more GMA contents in the microspheres resulted in higher decorating density of MNPs, with the maximum fraction of MP-60 reaching to 21 wt.%.

3.3. Comparison of the Two Routes. On the basis of the experimental results, polymer/magnetite raspberry-like structures could be rationally fabricated through the two pathways, in situ growth including solvothermal process and coprecipitation method, and interfacial immobilization methods containing electrostatic interactions. Because of the less effectiveness in tuning the structures of the microspheres, coprecipitation-reaction-based in situ growth route could not generate the desirable nanostructures for optimizing the further bioseparation applications. Compared with the coprecipitation reaction, solvothermal process was more effective in tuning the morphology of resultant composite microspheres. However, the solvothermal process required a long time reaction (>10 h) at an elevated temperature up to 200 °C, which was demonstrated to be time-consuming, costly and not suitable for mass production. Besides, multiplexed steps were involved in the process before the hybridization of MNPs and polymer. In contrast, electrostatic interaction based route was more time-saving with reaction period less than one hour, ready for manipulation, and powerful in structures constructions. Consequently, electrostatic-interaction-directed interfacial immobilization method was adopted as a desirable pathway in synthesizing PSG/Fe_3O_4 composite microspheres for further investigation in DNA separation.

3.4. Silica Coating onto the PSG-NH_2@Fe_3O_4 Composite Microspheres. To enhance the binding affinity toward DNA segments and aqueous dispersity, silica layer was coated onto the as-made PSG-NH_2@Fe_3O_4 composite microspheres by the modified stober method as reported.[29] Under ultrasonication condition, the precursor TEOS was hydrolyzed in a mixed ethanol and water solution of the seed microspheres and ammonia. Figure 7 showed the resultant silica-layer coated microspheres with increased amount of TEOS. With little dosage of 0.15 g TEOS in the case of 10 mg microspheres, raspberry-like morphology was maintained after the silica coating process (Figure 7a), and careful investigation on the

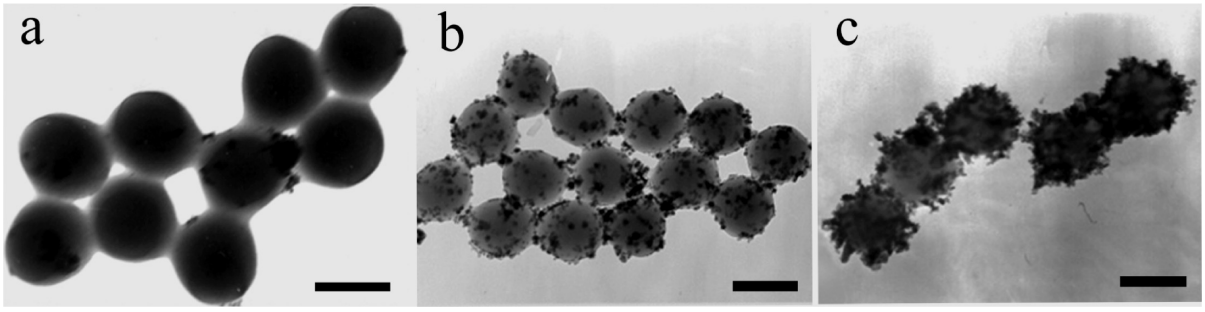

Figure 5. TEM images of PSG-NH_2@Fe_3O_4 composite microspheres obtained from PSG microspheres with GMA molar contents of (a) 20% (MP-20), (b) 40% (MP-40), and (c) 60% (MP-60). All scale bars are 200 nm.

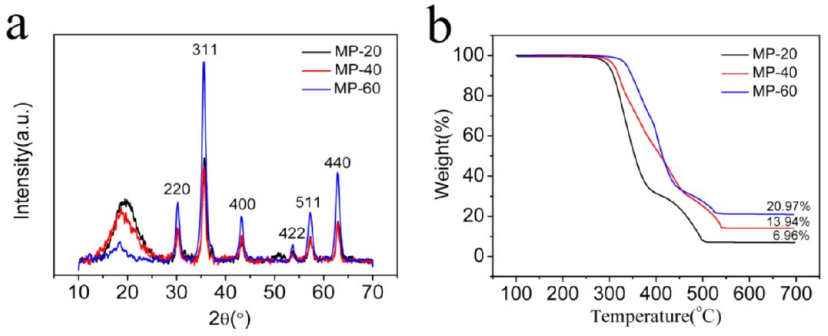

Figure 6. (a) Powder XRD patterns and (b) TG analysis of MP-20, MP-40, and MP-60.

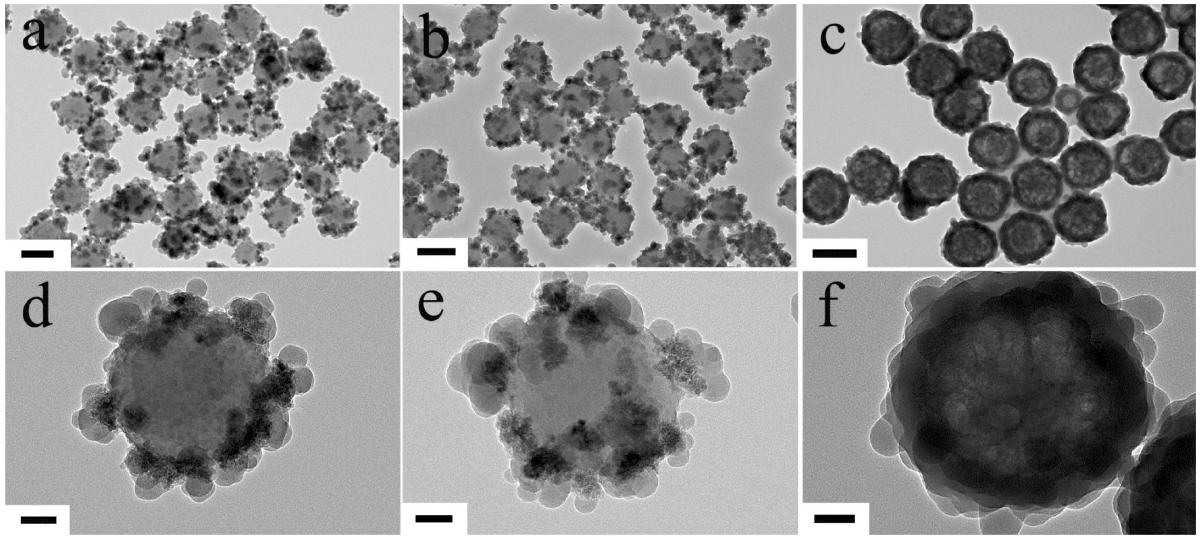

Figure 7. TEM images of PSG-NH_2@Fe_3O_4@SiO_2 composite microspheres with increased TEOS dosages of (a) and (d) 0.15 g, (b) and (e) 0.3 g, (c), and (f) 0.5 g in the case of 10 mg PSG-NH_2@Fe_3O_4 microspheres. The scale bars of panels a–c are 200 nm and those of d–f are 50 nm.

surface structure demonstrated that silica layers were formed around MNPs (Figure 7d), instead of covering the whole microspheres. The probable reason was that the MNPs with surface-capped carboxyl groups (−COOH) could serve as preferential anchoring sites for the nucleation and growth of silica nanoparticles. In addition, it was worth notice here that the silica-coated MNPs could still stayed on the surface of polymer microspheres during ultrasonication process, indicating the strong electrostatic interaction between the two components. Moreover, adding 0.3 g of TEOS to 10 mg microspheres led to composite structures with thicker silica layers (Figure 7b and 7e), the SEM image showed the raspberry-like structures of microspheres with relatively large surface-grown nodules after silica coating (Figure 8).[36] However, it was interesting here that, increasing the TEOS amount to 0.5 g (10 mg microspheres), adjacent silica nanoparticles were inclined to coalesce to form a continuous layer covering the whole PSG-NH_2@Fe_3O_4 microspheres with core–shell nanostructures (Figure 7c and 7f).

The silica layer of the magnetic composite microspheres was also demonstrated by FTIR spectra. From Figure 9a, it could be found that, compared with free PSG-NH_2, the spectrum of PSG-NH_2@Fe_3O_4 showed a strengthened absorbance around 586 cm^{-1}, which was indexed to the stretching vibration Fe–O bonding. After silica coating, obviously, intensified peaks were showed at 1090, 808, and 472 cm^{-1}, ascribing to the

dx.doi.org/10.1021/am301129n | ACS Appl. Mater. Interfaces 2012, 4, 4764–4775

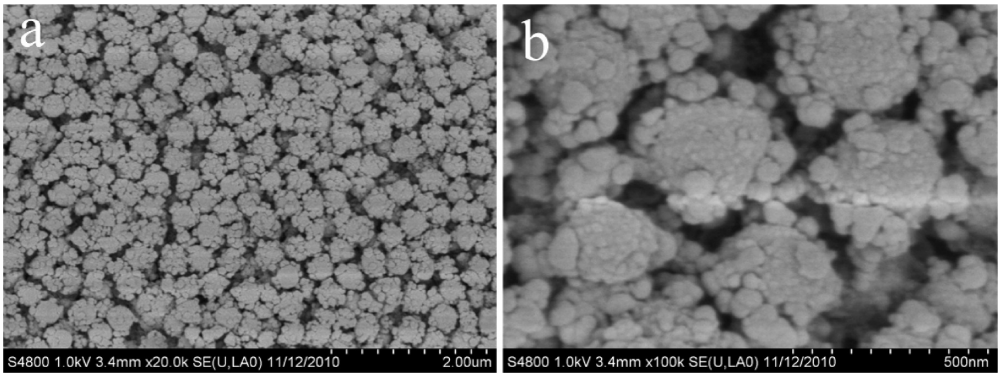

Figure 8. SEM images of PSG-NH_2@Fe_3O_4@SiO_2 composite microspheres with TEOS amount of 0.15 g in the case of 10 mg PSG-NH_2@Fe_3O_4 microspheres.

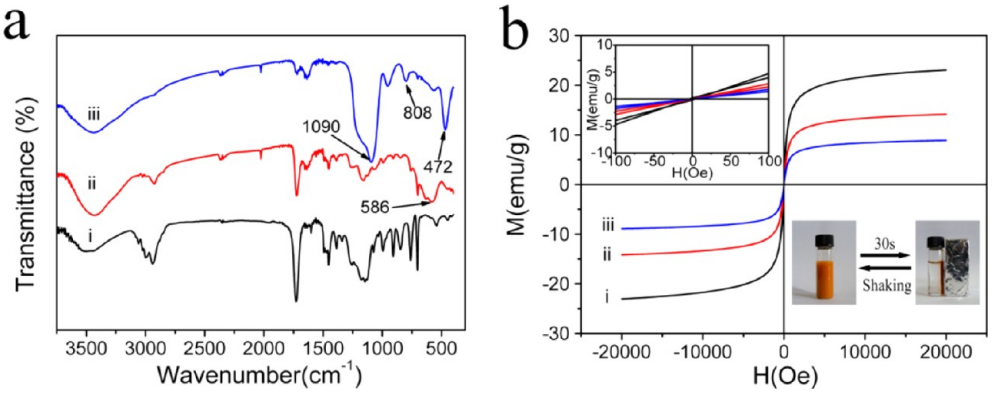

Figure 9. (a) FTIR spectra of (i) PSG-NH_2, (ii) PSG-NH_2@Fe_3O_4, (iii) PSG-NH_2@Fe_3O_4@SiO_2 (TEOS: 0.3 g) microspheres, and (b) magnetization curves of PSG-NH_2@Fe_3O_4@SiO_2 with different TEOS dosages of (i) 0.15 g, (ii) 0.3 g, and (iii) 0.5 g in the case of 10 mg PSG-NH_2@Fe_3O_4 microspheres.

characteristic unsymmetrical stretching vibration, symmetrical stretching vibration, and bending vibration of Si−O−Si, respectively. Meanwhile, the intensity of stretching vibration of Fe−O was reduced due to the silica coatings. Besides, magnetization curves revealed that PSG-NH_2@Fe_3O_4@SiO_2 microspheres owned a high saturation magnetization as much as 23.0 emu/g (Figure 9b) at 2T. To be more specific, the magnetic field intensity for bioseparation was approximate 1−1.5T, and the magnetization value of the as-made magnetic microspheres was about 21 emu/g, which could fulfill the requirement for bioseparation. The deviation between VSM data and TG result is probably because the saturation magnetization was not simply converted from the TG result due to the cross-linked polymer microspheres cannot completely decompose in the N_2 atmosphere. The magnetization values were decreased as the thickness of silica layers enhanced due to the less weight fraction of magnetic components. Moreover, from the insetting curves one could find that magnetic hysteresis loops could be negligible for the samples, indicating the superparamagnetic property of the products (300 K). Such an excellent paramagnetic property, together with the abundant surface charges (PSG-NH_2, +40.9 mV, PSG-NH_2@Fe_3O_4, −27.4 mV, PSG-NH_2@Fe_3O_4@SiO_2 (TEOS: 0.3 g), −22.0 mV), could help avoid the aggregation of magnetic microspheres and redisperse them easily after removal of external magnetic fields. The composite microspheres exhibited excellent colloidal dispersity and could be facilely isolated by an external magnet within 30 s, as shown in figure 9 inset.

3.5. Plasmid DNA Separation. Compared with the multistep-involved, time-consuming methods such as ultracentrifugation, hydroxyapatite chromatography, and ion-exchange chromatography,[37,38] separation of DNA, RNA, and other bioactive entities with magnetic silica composites is rather appealing for fundamental research and clinical diagnosis because of the convenience in mechanical sorting, trafficking, and micromanipulation simply by using an external magnetic field.[39,40] The strong capacity of silica components to bind DNA or RNA in the presence of high concentration of chaotropic reagents offers a rapid and efficient method to purify nucleic acid.[41]

The potential of PSG-NH_2@Fe_3O_4@SiO_2 composite microspheres to separate plasmid DNA was further investigated. Generally, plasmid DNA was initially extracted from the cultured *Escherichia coli* colony and separated with chromosomal DNA based on their differences of properties in the process of denaturalization. Agarose gel electrophoresis of the extracted samples exhibited characteristic patterns of plasmid DNA, and no legging or impure bands formed (Supporting Information Figure S4). The concentrations of the extracts in the elution solution were also calculated from UV−vis measurements (Supporting Information Table S3). Several results in Supporting Information Table S3 were over 2.0, suggesting that there were RNA contaminations in the samples. However, most of the values of A260/A280 were in the ranges of 1.8−2.1, demonstrating the plasmid DNA without protein, phenol, or other contaminants.[40]

Scheme 3. Schematic Illustration of PSG-NH_2@Fe_3O_4@SiO_2 Nanocomposites for Plasmid DNA Separation

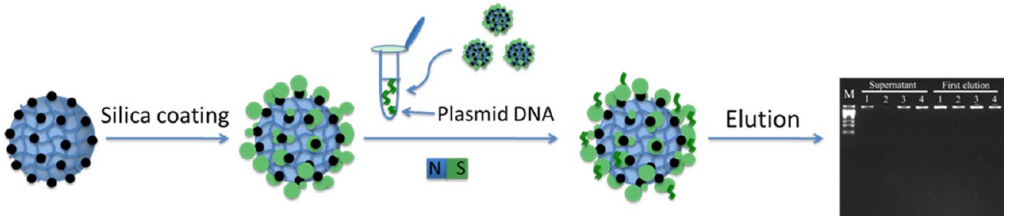

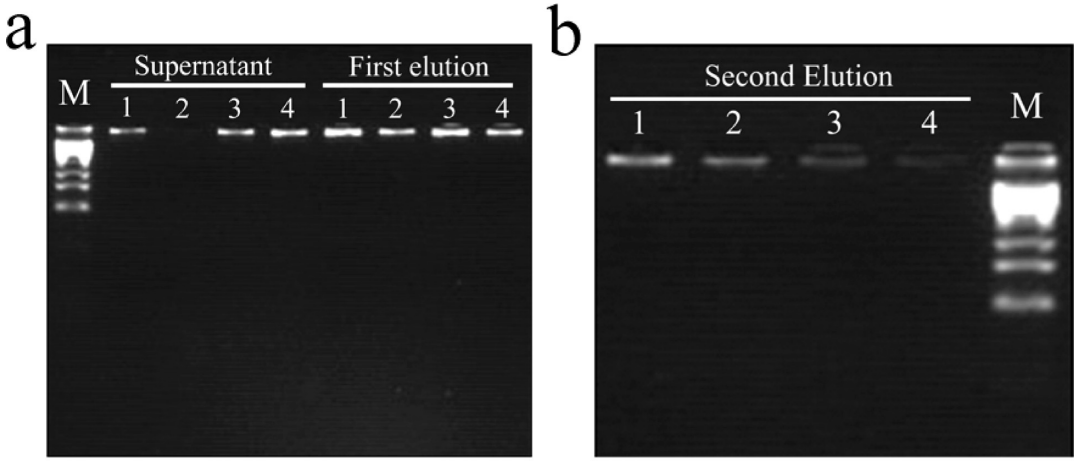

Figure 10. Agarose gel electrophoresis of plasmid DNA isolated by PSG-NH_2@Fe_3O_4@SiO_2 composite microspheres prepared with TEOS dosages of 0.15 g (lane 1), 0.3 g (lane 2), and 0.5 g (lane 3) in the case of 10 mg PSG-NH_2@Fe_3O_4 microspheres, commercial sample of SM1−015B (lane 4) at (a) first and (b) second elution.

Plasmid DNA separation experiments were performed using the PSG-NH_2@Fe_3O_4@SiO_2 samples. The samples were mixed with the SDS solution of plasmid DNA, separated by the external magnetic fields to the wall of a tube, then analyzed by agarose gel electrophoresis (Scheme 3), and quantified by UV−vis spectrometry. It was shown that the samples could effectively separate the targeted plasmid DNA from native solution and desorb them in elution (Figure 10a), while keeping structures of plasmid DNA intact during the processes. One issue needed notice here is that the agarose gel electrophoresis in lane 2 of Figure 10a may be seemingly inconsistent with the data in table 2 based on the UV−vis results. Since UV−vis measurement is a quantitative method to determine DNA concentration, the datum from UV−vis measurement is credible. In our experiment, the agarose gel electrophoresis was run for 20 min, which is similar to that as reported.[40] To better distinguish the supercoiled DNA from the open circular form one, the agarose gel probably need to be run for a longer time to give a nice DNA band. Generally, the band intensity of the supernatant after removal of the first three samples was weakened than that of commercially available SM1−015B, indicating the effectiveness of DNA isolation using the PSG-NH_2@Fe_3O_4 microspheres.

Table 2. Yield of Eluted Plasmid DNA from the PSG-NH_2@Fe_3O_4@SiO_2 Composite Microspheres and Comparison with the Standard Commercial Sample

	plasmid DNA (μg/mg)[b,c]			
sample[a]	first elution	second elution	total amount (μg/mg)	yield (%)
TEOS-0.15[d]	12.267	4.634	16.901	56.3
TEOS-0.3	12.047	1.310	13.357	44.5
TEOS-0.5	12.049	1.010	13.059	43.5
SM1-015B	6.800	0	6.800	22.7

[a]The dosage of sample is kept at 1 mg. [b]The amount of plasmid DNA is kept at 30 μg in each binding and eluting process. [c]The unit μg/mg represented the eluted amount (μg) of plasmid DNA from per mg of the samples. [d]TEOS-0.15 is denoted that sample 1 is PSG-NH_2@Fe_3O_4@SiO_2 microspheres prepared with TEOS dosage of 0.15 g in the case of 10 mg PSG-NH_2@Fe_3O_4 microspheres.

After the first elution, the equivalent extracted amounts of plasmid DNA for all the three composite microspheres could reach as high as 12 μg per mg (Table 2), approximately double the amount of that isolated by SM1−015B (6.8 μg/mg). Moreover, the intensity of band in lane 1 (first elution) corresponding to the plasmid DNA extraction with sample 1 (12.267 μg/mg, 0.15 g TEOS) was slightly stronger than that using sample 2 (12.047 μg/mg, 0.3 g TEOS) or sample 3 (12.049 μg/mg, 0.5 g TEOS). As for the second elution, compared with SM1−015B of none DNA extraction, the three samples could also separate certain amounts of plasmid DNA (Figure 10b). Combined with the two elution analysis, it was clear that the thinner the silica layer was (less TEOS dosage), the better plasmid DNA enrichment capacity resulted. The separation amounts increased from 13.059 μg/mg, 13.357 μg/mg to 16.901 μg/mg for TEOS-0.15, TEOS-0.3 and TEOS-0.5, respectively. Such tendency was probably ascribed to the relatively higher specific surface areas of samples with less silica coating. Importantly, the DNA separation capacities of the as-prepared sorbent were proved to be 2-fold more than that of the commercial-available sample of SM1−015B (6.800 μg/mg, 22.7% yield), further implying that the PSG-NH_2@Fe_3O_4@SiO_2 composite microspheres are superior to the commercial

dx.doi.org/10.1021/am301129n | ACS Appl. Mater. Interfaces 2012, 4, 4764−4775

counterparts in particular for bioseparations. Besides, our extraction method is a classical method for DNA extraction, the extracted DNA could well maintain its bioactivity for further application of genetic engineering or hybridization assay.[16,39]

4. CONCLUSION

In conclusion, polymer/magnetite/silica composite microspheres were rationally fabricated and served as nanoplatform for efficient separation of plasmid DNA. The synthetic procedure was performed as following steps: PSG microspheres were first prepared by surfactant-free emulsion polymerization, followed by surface functionlization to introduce carboxyl or amine groups. Then, the modified polymeric microspheres were covered by MNPs, either from the in situ growth pathway including solvothermal process and coprecipitation method, or from the interfacial immobilization route based on the electrostatic interaction. Through systematical comparisons, electrostatic interaction based heterodeposition method was demonstrated to be a facile and efficient way. Finally, the polymer/magnetite composite microspheres were coated with silica layer to promote binding affinity with plasmid DNA. The as-prepared structure-tunable PSG-NH_2@Fe_3O_4@SiO_2 microspheres revealed sustainable water dispersity, desirable saturation magnetization and excellent DNA separation capacity. The systematical investigation on the synthetic routes will undoubtedly shed light on the construction of more sophisticated nanostructures for the promising applications in DNA purification or other biorelated fields.

■ ASSOCIATED CONTENT

Supporting Information

TEM images, powder XRD pattern, and agarose gel electrophoresis. This material is available free of charge via the Internet at http://pubs.acs.org.

■ AUTHOR INFORMATION

Corresponding Author

*E-mail: ccwang@fudan.edu.cn.

Notes

The authors declare no competing financial interest.

■ ACKNOWLEDGMENTS

This work was supported by the National Science and Technology Key Project of China (2012AA020204), National Science Foundation of China (Grant Nos. 20974023, 21025519, 21128001, and 51073040).

■ REFERENCES

(1) Laurent, S.; Forge, D.; Port, M.; Boch, A.; Robic, C.; Elst, L. V.; Muller, R. N. *Chem. Rev.* **2008**, *108*, 2064−2110.
(2) Lu, A. H.; Salabas, E. L.; Schuth, F. *Angew. Chem., Int. Ed.* **2007**, *46*, 1222−1244.
(3) Gao, J. H.; Gu, H. W.; Xu, B. *Acc. Chem. Res.* **2009**, *42*, 1097−1107.
(4) Gao, L. Z.; Zhuang, J.; Nie, L.; Zhang, J. B.; Zhang, Y.; Gu, N.; Wang, T. H.; Feng, J.; Yang, D. L.; Perrett, S.; Yan, X. Y. *Nat. Nanotechnol.* **2007**, *2*, 577−583.
(5) Ge, J. P.; Huynh, T.; Hu, Y. X.; Yin, Y. D. *Nano Lett.* **2008**, *8*, 931−934.
(6) Cheng, K.; Peng, S.; Xu, C. J.; Sun, S. H. *J. Am. Chem. Soc.* **2009**, *131*, 10637−10644.
(7) Luo, B.; Xu, S.; Ma, W. F.; Wang, W. R.; Wang, S. L.; Guo, J.; Yang, W. L.; Hu, J. H.; Wang, C. C. *J. Mater. Chem.* **2010**, *20*, 7107−7113.
(8) Deng, Y. H.; Qi, D. W.; Deng, C. H.; Zhang, X. M.; Zhao, D. Y. *J. Am. Chem. Soc.* **2008**, *130*, 28−29.
(9) Gu, H. W.; Xu, K. M.; Xu, C. J.; Xu, B. *Chem. Commun.* **2006**, *42*, 941−949.
(10) Lee, H.; Yoon, T.; Weissleder, R. *Angew. Chem., Int. Ed.* **2009**, *48*, 5657−5660.
(11) Xu, S.; Ma, W. F.; You, L. J.; Li, J. M.; Guo, J.; Hu, J. J.; Wang, C. C. *Langmuir* **2012**, *28*, 3271−3278.
(12) Deng, Y. H.; Cai, Y.; Sun, Z. K.; Liu, J.; Liu, C.; Wei, J.; Li, W.; Liu, C.; Wang, Y.; Zhao, D. Y. *J. Am. Chem. Soc.* **2010**, *132*, 8466−8473.
(13) Ge, J. P.; Hu, Y. X.; Zhang, T. R.; Yin, Y. D. *J. Am. Chem. Soc.* **2007**, *129*, 8974−8975.
(14) Liu, J.; Qiao, S. Z.; Hu, Q. H.; Lu, G. Q. *Small* **2011**, *7*, 425−443.
(15) Bao, J.; Chen, W.; Liu, T. T.; Zhu, Y. L.; Jin, P. Y.; Wang, L. Y.; Liu, J. F.; Wei, Y. G.; Li, Y. D. *ACS Nano* **2007**, *1*, 293−298.
(16) Zhao, X.; Tapec-Dytioco, R.; Wang, K.; Tan, W. *Anal. Chem.* **2003**, *75*, 3476−3483.
(17) Ma, W. F.; Zhang, Y.; Li, L. L.; You, L. J.; Zhang, P.; Zhang, Y. T.; Li, J. M.; Yu, M.; Guo, J.; Lu, H. J.; Wang, C. C. *ACS Nano* **2012**, *6*, 3179−3188.
(18) Leslie, D. C.; Li, J. Y.; Strachan, B. C.; Begley, M. R.; Finkler, D.; Bazydlo, L. A. L.; Barker, N. S.; Haverstick, D. M.; Utz, M.; Landers, J. P. *J. Am. Chem. Soc.* **2012**, *134*, 5689−5696.
(19) Chen, H. M.; Deng, C. H.; Zhang, X. M. *Angew. Chem., Int. Ed.* **2010**, *49*, 607−611.
(20) Sauzedde, F.; Elaissari, A.; Pichot, C. *Colloid Polym. Sci.* **1999**, *277*, 846−855.
(21) Kawaguchi, H.; Fujimoto, K.; Nakazawa, Y.; Sakagawa, M.; Ariyoshi, Y.; Shidara, M.; Okazaki, H.; Ebisawa, Y. *Colloids Surf., A: Physicochem. Eng. Aspects* **1996**, *109*, 147−154.
(22) Mu, B.; Liu, P.; Dong, Y.; Lu, C. Y.; Wu, X. L. *J. Polym. Sci., Part A: Polym. Chem.* **2010**, *48*, 3135−3144.
(23) Zhang, F.; Wang, C. C. *Langmuir* **2009**, *25*, 8255−8262.
(24) Du, P. C.; Liu, P.; Mu, B.; Wang, Y. J. *J. Polym. Sci., Part A: Polym. Chem.* **2010**, *48*, 4981−4988.
(25) Huang, Z. B.; Tang, F. Q. *J. Colloid Interface Sci.* **2004**, *275*, 142−147.
(26) Caruso, F.; Susha, A. S.; Giersig, M.; Mohwald, H. *Adv. Mater.* **1999**, *11*, 950−953.
(27) Caruso, F.; Spasova, M.; Susha, A.; Giersig, M.; Caruso, R. A. *Chem. Mater.* **2001**, *13*, 109−116.
(28) Song, X. J.; Hu, J.; Wang, C. C. *Colloids Surf., A: Physicochem. Eng. Aspects* **2011**, *380*, 250−256.
(29) Luo, B.; Song, X. J.; Zhang, F.; Xia, A.; Yang, W. L.; Hu, J. H.; Wang, C. C. *Langmuir* **2010**, *26*, 1674−1679.
(30) Deng, H.; Li, X. L.; Peng, Q.; Wang, X.; Chen, J. P.; Li, Y. D. *Angew. Chem., Int. Ed.* **2005**, *44*, 2782−2785.
(31) Xuan, S. H.; Wang, Y. X. J.; Yu, J. C.; Leung, K. C. F. *Chem. Mater.* **2009**, *21*, 5079−5087.
(32) Xu, S.; Luo, Z. M.; Han, Y. J.; Guo, J.; Wang, C. C. *RSC Adv.* **2012**, *2*, 2739−2742.
(33) Luo, B.; Xu, S.; Luo, A.; Wang, W. R.; Wang, S. L.; Guo, J.; Lin, Y.; Zhao, D. Y.; Wang, C. C. *ACS Nano* **2011**, *5*, 1428−1435.
(34) Chen, Q.; Rondinone, A. J.; Chakoumakos, B. C.; Zhang, Z. J. *J. Magn. Magn. Mater.* **1999**, *194*, 1−7.
(35) Liu, C. Y.; Guo, J.; Yang, W. L.; Hu, J. H.; Wang, C. C.; Fu, S. K. *J. Mater. Chem.* **2009**, *19*, 4764−4770.
(36) Agrawal, M.; Gupta, S.; Stamm, M. *J. Mater. Chem.* **2011**, *21*, 615−627.
(37) Li, F. S.; Goessler, W.; Irgolic, K. J. *J. Chromatogr. A* **1999**, *830*, 337−344.
(38) Gilar, M. *Anal. Biochem.* **2001**, *298*, 196−206.
(39) Stoeva, S. I.; Huo, F. W.; Lee, J. S.; Mirkin, C. A. *J. Am. Chem. Soc.* **2005**, *127*, 15362−15363.

(40) Shao, D. D.; Xia, A.; Hu, J. H.; Wang, C. C.; Yu, W. M. *Colloids Surf., A: Physicochem. Eng. Aspects* **2008**, *322*, 61−65.
(41) Gai, L. G.; Li, Z. L.; Hou, Y. H.; Jiang, H. H.; Han, X. Y.; Ma, W. Y. *J. Phys. D: Appl. Phys.* **2010**, *43*, 1−8.